JOURNAL OF PHYSICAL ORGANIC CHEMISTRY
*J. Phys. Org. Chem.* **12**, 171–175 (1999)

# Dimer formation of a stilbenesulphonic acid salt in aqueous solution

**Jan Alsins,[1] Mikael Björling,[2]* István Furó[2] and Valdis Egle[1]†**

[1]University of Uppsala, Department of Physical Chemistry, P.O. Box 532, SE-751 21 Uppsala, Sweden
[2]Royal Institute of Technology, Physical Chemistry, SE-100 44 Stockholm, Sweden

*Received 8 January 1998; revised 30 April 1998; accepted 30 April 1998*

ABSTRACT: The steady-state and time-resolved fluorescence and $^1$H NMR spectra of a stilbenesulphonic acid salt, commonly used as an optical brightening agent, was studied as a function of concentration in aqueous solution. The aggregates, formed at higher concentrations, were shown to be predominantly dimers with the central stilbene moieties of the molecules stacked plane-parallel. The equilibrium constant for the dimer formation at 25 °C was obtained from both NMR and fluorescence measurements. Copyright © 1999 John Wiley & Sons, Ltd.

KEYWORDS: Stilbenesulphonic acid salt; dimer formation; fluorescence; NMR

## INTRODUCTION

The salts of *trans*-stilbenesulphonic acids are widely used in industrial applications as fluorescent brightening and whitening agents. In the following they will be collectively referred to as optical brightening agents (OBAs). The optical brightening agents act by absorbing light in the invisible near-UV region and re-emitting it as blue fluorescence with high yield. The addition of this light to the daylight reflected from an object is perceived as an increase of the brightness[1] of the object. The relative deficiency of blue light in the reflected light from yellowish objects, e.g. natural fibres, is compensated for by the addition of the blue fluorescence which is perceived as an increase of the whiteness[1] of the object.

At high loads of OBA, a loss of the desired whitening effect, perceived as a greyish or a greenish hue, is often observed. This phenomenon is well known in paper-making where the quality in this respect is monitored with brightness measurements.[2,3] It has been suggested[3] that the greying and greening effects are due to multiple adsorption of OBAs on the adsorption sites on, for example, cellulose fibres, i.e. to the formation of bound OBA aggregates. A similar spectral shift of the fluorescence spectrum towards longer wavelengths can be observed upon increasing the concentration of OBA in aqueous solution. In order to gain insight into the underlying physical mechanisms of the greying and greening effects, the properties of OBA in aqueous solution were studied.

In this paper, the concentration-dependent properties of a commonly used water-soluble stilbenesulphonic acid OBA (**I**; Fig. 1) were investigated by both fluorescence and NMR techniques. Considering the above observations, fluorescence spectroscopy is a natural choice for the study. Changing the concentration also alters the $^1$H NMR spectrum of **I** primarily by shifting the observed proton lines from the stilbene moiety. Therefore, $^1$H NMR spectroscopy was chosen as a second independent method.

Dye molecules in aqueous solution have been extensively studied,[4–15] primarily by absorption spectroscopy.[4–10] The observed spectral changes with increasing concentration are generally interpreted in terms of the

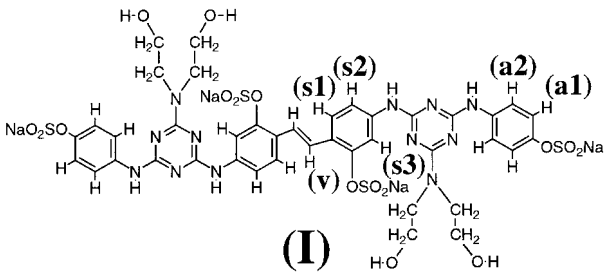


**Figure 1.** Structure of the studied stilbene derivative **I**. The labels on the aromatic protons, on the right-hand side of the symmetrical molecule, correspond to the assignment of NMR peaks in Fig. 4

**Correspondence to:* M. Björling, Royal Institute of Technology, Physical Chemistry, SE-100 44 Stockholm, Sweden.
E-mail: mikaelb@physchem.kth.se
†*Permanent address:* Latvian State Institute of Wood Chemistry, Dzerbenes iela 27, LV-1006 Riga, Latvia.
*Contract/grant sponsor:* Swedish Cellulose and Paper Research Foundation.
*Contract/grant sponsor:* Swedish Natural Science Research Council (NFR).
*Contract/grant sponsor:* Swedish Institute.


CCC 0894–3230/99/030171–05 $17.50

self-association of the dye molecules into dimers, trimers and higher order aggregates.[5–15] More recently, $^1$H NMR spectroscopy has been employed to study dye aggregation.[11–15] In previous studies, the aggregation of planar organic dyes has often been found to follow an isodesmic model[5,8–13] (where each step towards higher aggregates proceeds with the same equilibrium constant), but dimer formation has also been reported.[5–7,9,14,15] The results shown below indicate that the aggregates of **I** are predominantly dimers at the concentrations studied.

## EXPERIMENTAL

The stilbene derivative **I**, the sodium salt of 4,4′-bis[4-(*p*-sulphoanilino)-6-*NN*-bis(*β*-hydroxyethyl)amino-1,3,5-triazin-2-yl]amino *trans*-stilbene-2,2′-disulphonic acid,[16] MW = 1133, was a complimentary sample from Ciba Specialty Chemicals. The sample was an amorphous powder containing 85 wt% of **I**, the remainder being mainly sodium chloride, moisture and minute amounts of unreacted *N*,*N*-bis(*β*-hydroxyethyl)amine.

Solutions for fluorescence measurements were prepared with deionized water and experiments were carried out in equilibrium with the atmosphere at 25 °C, unless stated otherwise. Fluorescence spectra were recorded on a SPEX Fluorolog 212 spectrometer, with photon counting detection, in front face geometry with 1 mm quartz cells, with excitation at 350 nm. To avoid photolytic changes of the sample (due to *trans–cis* isomerisation of the stilbene moiety[17–20]), the excitation slits were set at 0.1 mm and the emission spectrum was scanned rapidly. Two consecutive runs gave the same spectrum within the limits of noise. Time-resolved fluorescence decays at selected wavelengths were recorded with a pulsed picosecond Nd:YAG laser system, with frequency doubling, exciting at 320 nm with 200–500 ps pulses depending on the adjustment of the system.[21] Adsorption spectra were recorded on a Cary Model 2400 UV–VIS–NIR spectrometer or a Hewlett-Packard Model 8453 diode-array spectrophotometer.

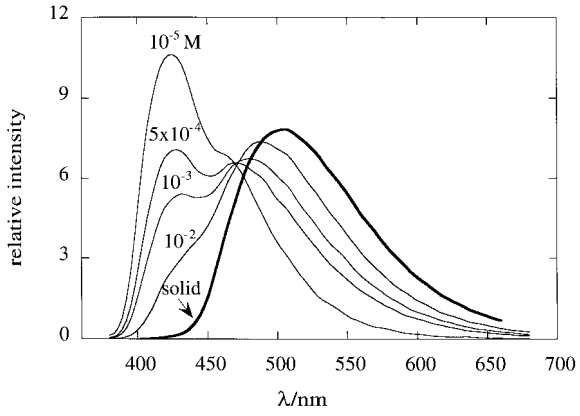


**Figure 2.** Fluorescence spectra of **I** at selected concentrations in aqueous solution and of the solid. For comparison the spectra have been normalized to equal areas (this normalization was chosen owing to a lack of normalizing parameters for the solid sample)

Solutions for NMR measurements were prepared with $D_2O$ (99.9%) purchased from Isotec (Miamisburg, OH, USA). The solutions were carefully protected from exposure to light. The $^1$H NMR spectra were obtained at 25 °C on a Bruker AMX-300 spectrometer. To prevent the comparatively strong water signal from obscuring the peaks from **I,** the former was suppressed using a long, low-level presaturation pulse. The assignment of the $^1$H resonances was provided by 2D COSY spectroscopy (results not shown), which allows all features to be accounted for. All chemical shifts were referenced to internal TMS.

## RESULTS AND DISCUSSION

### Fluorescence

Fluorescence spectra recorded at different concentrations of **I** in aqueous solution and from the pure compound, powder of **I**, are shown in Fig. 2. The spectrum at $10^{-5}$ M has a broad maximum at 418 nm and does not change features on dilution to $10^{-6}$ and $10^{-7}$ M. It can therefore be considered as the fluorescence spectrum of the monomer of **I**. With increasing concentration the fluorescence spectra gradually change. In the concentration range $5 \times 10^{-4}$–$1 \times 10^{-3}$ M the spectra are intermediate, and from $5 \times 10^{-3}$ M upwards they are almost independent of concentration (apart from the effect of the re-absorption of fluorescence light due to the overlap between absorption and emission bands). The high-concentration spectra are strongly shifted towards the spectrum of solid OBA. We ascribe this shift to aggregation. Thus, the solution spectrum at $10^{-2}$ M in Fig. 2 predominantly represents aggregates. The greenish emission from aggregated OBA, the broad maximum at 495 nm, causes the greening effect.

The time dependence of the fluorescence decay at three selected wavelengths in a $10^{-3}$ M solution is presented in Fig. 3. At this concentration, the spectrum is intermediate, with both monomers (*M*) and aggregates ($A_n$) of **I**. The decays are biphasic and fit to two first-order decays with lifetimes of 0.5 and 12 ns, respectively. The lifetime for the fast decay is at the time resolution of the instrument and is estimated to be 0.5 ns or less. The fast component dominates at short wavelengths where the monomer emission is dominant and is strongly reduced at longer wavelengths where the slow component dominates. Only the fast decay was present in a $10^{-5}$ M solution where only monomers exist. We therefore ascribe the fast component to excited monomers *M** and the slow component to excited aggregates.

Before further use of the fluorescence data, it is

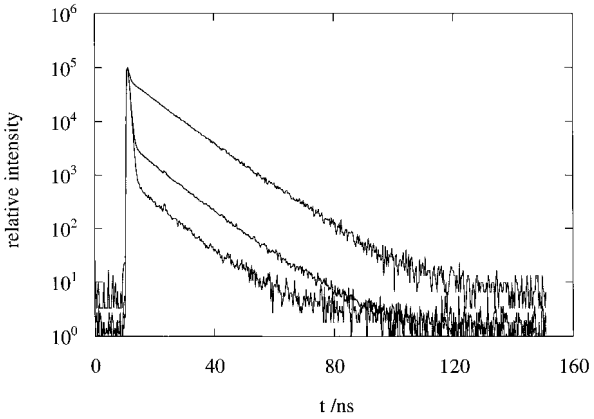


**Figure 3.** Fluorescence decays of **I** in $10^{-3}$ M solution at three selected wavelengths, 400, 420 and 560 nm, from the bottom upwards. The spectra are normalized to the same peak intensity. The fast component dominates at short wavelengths and is strongly reduced (in relation to the slow component) at 560 nm

important to consider two possible mechanisms for the formation of excited aggregates $A_n$*. The first is the direct excitation of the ground-state aggregate:

$$A_n + h\nu = A_n^* \tag{1}$$

and the second is the diffusion-controlled formation of excimers $A_n$*:

$$M + h\nu = M^*$$

$$M^* + A_{n-1} = A_n^* \tag{2}$$

To distinguish between the two mechanisms, the excimer formation rate of pyrene, being a smaller and more rapidly diffusing molecule than **I**, may be taken as an upper bound for the excimer formation rate of **I** by Eqn (2). Birks *et al.*[22] found that the rate constant for pyrene excimer formation in degassed hexane at 25 °C was $6.7 \times 10^9$ M$^{-1}$ s$^{-1}$. The maximum pseudo-first-order disappearance rate of *M** by reaction (2) in a $10^{-3}$ M solution (as in Fig. 3) would then be $6.7 \times 10^6$ s$^{-1}$, corresponding to a half-life of 103 ns. However, the lifetime for the fluorescence decay of *M** was estimated experimentally to be of the order of 0.5 ns (i.e. the half-life is 0.3 ns) and therefore *M** decays to the ground state before any appreciable formation of excimers by reaction (2). Hence the slow decay is associated with the direct excitation of ground-state aggregates by reaction (1) and the concentrations of *M** and $A_n$* are proportional to the ground-state concentrations of *M* and $A_n$, respectively.

We now return to Fig. 2 and the iso-emissive point at 470 nm found for the normalized solution spectra. It indicates a transformation between two species, i.e. monomers and one type of aggregate. Since the isodesmic model implies the co-existence of consecutive higher aggregates, a dimerization equilibrium ($n = 2$) is supported, that is,

$$M + M = D \tag{3}$$

where *M* and *D* represent the monomer and the dimer, respectively.

Furthermore, the first-order aggregate decay in Fig. 3 provides an additional strong indication for dimer formation. The decay from the solid (not shown) is strongly non-exponential and a factor of two slower than the aggregate decay. Plausibly, the higher the aggregates, the longer are the fluorescence lifetimes. Thus, a sizeable aggregate polydispersity would lead to deviations from a first-order decay, i.e. instead of the decays shown in Fig. 3, linear for about 12 half-lifes, curved decays would be observed.

## Absorption

The adsorption spectrum of **I** was blue-shifted upon increasing the concentration, i.e. on aggregation of **I**. According to the molecular exciton theory,[23] this suggests that the transition dipoles of the molecules in the dimer are arranged in plane-parallel, sandwich (H-type) aggregates.

Owing to the efficient light-induced conversion of **I** in solution to the non-fluorescent *cis*-stilbene isomer,[17–20] we did not use absorption measurements further.

## Nuclear magnetic resonance

The concentration-dependent distribution of **I** between monomers and dimers can also be conveniently investigated using the observed concentration dependence of the $^1$H NMR chemical shifts. The $^1$H NMR spectra of the aromatic protons presented in Fig. 4 for high and low concentrations show a general upfield shift upon decreasing the concentration. The shift is largest for protons *v*, *s1* and *s2* (see Fig. 1 for assignment). The spectra are of the fast exchange type with no splitting of the lines between dimers and monomers. Therefore, the observed chemical shift at a given concentration is the simple statistical average:

$$\delta_{obs} = P_D\delta_D + (1 - P_D)\delta_M \tag{4}$$

where $\delta_{obs}$ is the observed chemical shift, $\delta_M$ and $\delta_D$ are the shifts corresponding to the monomer and dimer state, respectively, and $P_D$ is the probability of finding a molecule in the dimer state. The assumptions behind this approach are that all investigated samples are sufficiently dilute that all shift changes are caused by the aggregation process and not by statistical intermolecular interactions (clearly satisfied in our system) and that there are unique chemical shifts corresponding to the monomer and dimer states. The monomer and dimer shifts probably differ because of the aromatic shift effects[11,13–15,23–25] exerted

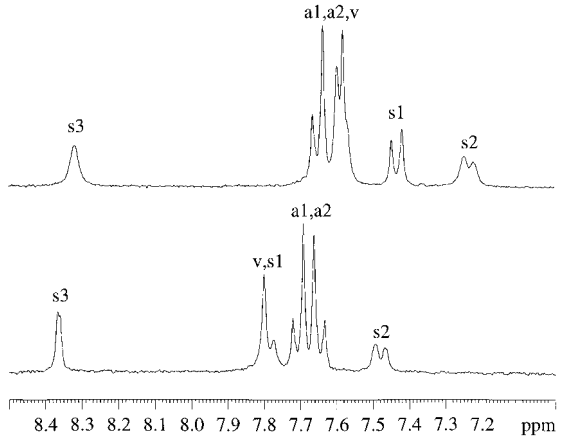


**Figure 4.** $^1$H NMR spectra of **I** dissolved in $D_2O$. The upper spectrum is from an $8 \times 10^{-3}$ M solution (recorded with eight scans) and the lower spectrum is from a $2 \times 10^{-4}$ M solution (512 scans). The chemical shifts of *s1*, *s2*, and $\nu$ (see Fig. 1) are strongly concentration dependent, whereas those of *s3*, *a1*, and *a2* are only weakly so

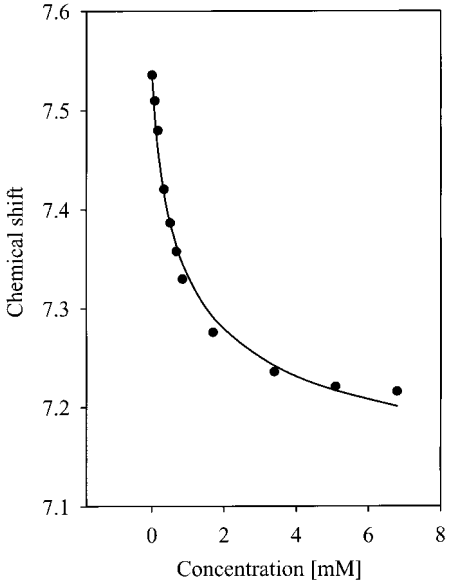


**Figure 5.** The fit to Eqn (6) of the observed concentration dependence of the chemical shift of *s2*. The accuracy of the experimental chemical shifts is ±0.002 ppm, with the exception of the three lowest concentrations, where it is ±0.004 ppm

by the ring currents in one molecule of the dimer on the protons of the other molecule. This also means that the magnitudes of the concentration-dependent shifts within the molecule may vary widely, as is observed.

The fact that the $\nu$, *s1*, and *s2* protons are strongly affected, whereas *a1* and *a2* are only weakly affected, indicates that the central stilbene moieties of the aggregating molecules are closer to each other in the dimer than the outer aniline rings. The planar conformation of *trans*-stilbene facilitates such an arrangement,[26,27] with the outer aniline rings either tilted or bent away from each other.

Unfortunately, most peaks in the aromatic region partly or fully overlap, which prevents us from accurately determining the concentration dependence of their $^1$H chemical shifts. Only *s2* and *s3* are clearly separated in the whole concentration range, *s2* being the most shifted. Therefore, the concentration dependence of the *s2* chemical shift will be used to estimate the equilibrium constant.

Most observed lines are broader at higher than at lower concentrations. While this broadening predominantly may be a dynamic effect (i.e. due to a slower tumbling of the dimer), the magnitude of the observed broadening for the line with the strongest concentration dependence of the chemical shift (i.e. *s2*) nevertheless provides a conservative upper limit for the lifetime. Thus, in the range 2–10 mM where the monomer-to-dimer ratio is roughly constant (0.3–0.5), the extra broadening of about 10 Hz (with respect to the *s2* line in the spectrum at $10^{-5}$ M) yields $\tau_D < 100$ μs.[28]

## Equilibrium constant

The equilibrium constant $K$ for the dimer formation according to reaction (3) is given by

$$K = \frac{x}{(c - 2x)^2} \tag{5}$$

where $c$ is the total concentration of **I** and $x$ is the concentration of dimers at equilibrium. Solving for $x$ in terms of $K$ and $c$, using Eqn (4) and $P_D = 2x/c$ (since there are two molecules in each dimer), the expected concentration dependence of the chemical shift is given by

$$\delta_{obs} = \delta_D + (\delta_D - \delta_M)\frac{(1 - \sqrt{8Kc + 1})}{4Kc} \tag{6}$$

Since the fluorescence measurements show that a $10^{-5}$ M solution contains only monomers, the chemical shift of *s2* in the monomer state may be fixed at $\delta_M \approx 7.54$. A fit of the observed concentration dependence of the *s2* chemical shift, using $K$ and $\delta_D$ as free parameters, is shown in Fig. 5. The equilibrium constant obtained is $K = 725 \pm 97$ M$^{-1}$. Using this $K$ and Eqn (5), 77% of the molecules should participate in dimers at $10^{-2}$ M. We note that a fit to an isodesmic model of aggregation (under the unsubstantiated extra assumption that the chemical shifts are independent of aggregate size) is equally fair, so the dimer formation could not have been safely established based solely on the chemical shift data.

A similar analysis was used to estimate the equilibrium constant from the fluorescence data at five wavelengths, 420, 490, 530, 550 and 570 nm, by substituting the normalized (to unit of absorbed light) intensities for the chemical shifts in Eqn (6). The average value obtained of $K = (1.2 \pm 0.5) \times 10^3$ M$^{-1}$ agrees (within error limits)

with the value obtained by NMR spectroscopy. When comparing the equilibrium constants from fluorescence and NMR measurements one should note that $K$ may differ in $H_2O$ and $D_2O$, respectively.[10] The errors of the individual fluorescence estimates are large and comparable to the scatter of the equilibrium constants obtained using different wavelengths.

Even though the fit in Fig. 5 is fairly good, the experimental points clearly level off more quickly than the theoretical expression in Eqn (6). However, an implicit assumption is that $K$ is independent of the total concentration $c$. Since one of the main obstacles to the dimer formation of **I** must be the electrostatic repulsion between the sulphonate groups, $K$ should depend on the ionic strength. Since **I** itself is a salt and since the remainder of the sample is mainly sodium chloride, the ionic strength (and consequently $K$) should increase with increasing total concentration, thus producing the observed experimental trend [i.e. a faster levelling-off than expected from Eqn (6)]. (Note that the ionic strength at the lowest and the highest concentration of **I** differs by a factor of 103) Further studies at higher constant ionic strengths should clear up this point.

## CONCLUSIONS

The observed changes in the fluorescence and $^1$H NMR spectra upon increasing the concentration of **I** in aqueous solution are interpreted in terms of self-association into dimers at the concentrations studied. The formation of dimers is strongly supported by the iso-emissive point in Fig. 2, and also the biphasic fluorescence decay in Fig. 3, where the slow component clearly is unimodal. Dimer formation of **I** is also consistent with the concentration dependence of the NMR line shifts and the approximate agreement of the equilibrium constants evaluated at different wavelengths (Fig. 2).

The equilibrium constants for dimer formation in $D_2O$ and $H_2O$, obtained from the $^1$H NMR and fluorescence measurements, are $725 \pm 97$ and $(1.2 \pm 0.5) \times 10^3$ M$^{-1}$, respectively. The largest chemical shifts, due to the aromatic ring currents of the other molecule in the dimer, are observed for the protons *s1*, *s2*, and $\nu$, indicating that the stilbene moieties are close. This is in line with the plane-parallel stacking of the chromophores suggested by the application of the exciton model to the concentration-induced blue shift in the absorption spectra of **I**. The fluorescence and NMR data limit (from below and from above, respectively) the lifetime of a dimer to $10^{-8}$ s $< \tau_D < 10^{-4}$ s in the concentration range 2–10 nM.

## Acknowledgements

The Swedish Cellulose and Paper Research Foundation (J.A.), the Swedish Natural Science Research Council (NFR) (I.F.) and the Swedish Institute (V.E.) are thanked for financial support.

## REFERENCES

1. M. Zahradník, The Production and Application of Fluorescent Brightening Agents, pp. 28–29 Wiley, Chichester (1982).
2. A. J. Ragauskas, Surface Analysis of Paper, edited by T. E. Conners and S. Banerjee, pp. 109–118 CRC Press, Boca Raton, FL (1995).
3. F. Mueller, D. Loewe and B. Hunke, *Wochenbl. Papierfabr.* **119**, 191–196 (1991).
4. S. E. Sheppard, *Proc. R. Soc. London, Ser. A* **82**, 256 (1909).
5. E. Rabinowitch and L. F. Epstein, *J. Am. Chem. Soc.* **63**, 69–78 (1941).
6. V. Z. Zanker, *Phys Chem. (Leipzig)* **199**, 225 (1952); **200**, 250 (1952).
7. G. R. Haugen and W. H. Meluish, *Trans. Faraday Soc.* **60**, 386–394 (1964).
8. M. E. Lamm and D. M. Neville Jr, *J. Phys. Chem.* **69**, 3872 (1965).
9. E. H. Braswell, *J. Phys Chem.* **88**, 3653–3658 (1984).
10. S. Das, G. Thomas, K. J. Thomas, V. Madhavan, D. Liu, V. K. Prashant and M. V. George, *J. Phys. Chem.* **100**, 17310–17315 (1996).
11. D. J. Blears and S. S. Danyluk, *J. Am. Chem. Soc.* **88**, 1084–1085 (1966); **89**, 21–26 (1967).
12. J. L. Dimicoli and C. Hélène, *J. Am. Chem. Soc.* **95**, 1036–1044 (1973).
13. T. Asakura and M. J. Ishida, *Colloid Interface Sci.* **130**, 184–189 (1989).
14. P. Ilich, P. K. Mishra, S. Macura and T. P. Burghardt, *Spectrochim. Acta, Part A* **52**, 1323–1330 (1996).
15. K. Kano, H. Minamizono, T. Kitae and S. Negi, *J. Phys. Chem. A* **101**, 6118–6124 (1997).
16. M. Okawara, T. Kitao, T. Hirashima and M. Matsuoka, Organic Colorants, Physical Sciences Data, Vol. **35**, pp. 58–59 Elsevier, Tokyo (1988).
17. R. M. Hochstrasser, *Pure Appl. Chem.* **52**, 2683–2691 (1980).
18. J. Saltiel and Y.-P. Sun in Photochromism. Molecules and Systems, edited by H. Durr and H. Bouas-Laurent, pp. 64–164 Elsevier, Amsterdam (1990).
19. D. H. Waldeck, *Chem. Rev.* **91**, 415–436 (1991).
20. T. Arai and K. Tokumaru, *Chem. Rev.* **93**, 23–39 (1993).
21. B. Medhage, M. Almgren, J. Alsins, *J. Phys. Chem.* **97**, 7753–7762 (1993).
22. J. B. Birks, D. J. Dyson and I. H. Munro, *Proc. R. Soc. London, Ser. A* **275**, 575–588 (1963).
23. M. Kasha, H. R. Rawls and A. El-Bayoumi, *Pure Appl. Chem.* **11**, 371 (1965).
24. C. E. Johnson Jr and F. A. Bovey, *J. Chem. Phys.* **29**, 1012–1014 (1958).
25. J. A. Pople, W. G. Schneider and H. J. Bernstein, High-Resolution Nuclear Magnetic Resonance, Chapt. 16. McGraw-Hill, New York (1959).
26. C. H. Choi and M. Kertesz, *J. Phys Chem. A* **101**, 3823–3831 (1997).
27. V. Molina, M. Merchán and B. O. Roos, *J. Phys. Chem. A* **101**, 3478–3487 (1997).
28. R. R. Ernst, G. Bodenhausen and A. Wokaun, Principles of Nuclear Magnetic Resonance in One and Two Dimensions Clarendon Press, Oxford (1987).